Progress in Organic Coatings 119 (2018) 155–163

Contents lists available at ScienceDirect

Progress in Organic Coatings

journal homepage: www.elsevier.com/locate/porgcoat

Long-lasting isothiazolinone-based biocide obtained by encapsulation in micron-sized mesoporous matrices

Lucas E. Mardones[a], María S. Legnoverde[a,b], Andrea M. Pereyra[a,b], Elena I. Basaldella[a,*]

[a] Centro de Investigación y Desarrollo en Ciencias Aplicadas (CINDECA), Facultad de Ciencias Exactas, Universidad Nacional de La Plata – CONICET Calle 47N°257, B1900AJK La Plata, Argentina

[b] Universidad Tecnológica Nacional, Facultad Regional La Plata, 124 y 60, 1900 La Plata, Argentina

ARTICLE INFO

Keywords:
Mesoporous silicas
Adsorption
Controlled release
Biocides
Isothiazolinones

ABSTRACT

The use of mesoporous silica materials as new hosts for stabilizing isothiazolinone-based biocides was investigated. Two types of porous matrices were synthesized: SBA-15 mesoporous silica and mesocellular siliceous foam (MCF). The physicochemical properties of the silicas (structure, textural properties) were evaluated by SEM, TEM, XRD and adsorption/desorption of N_2 in order to determine their ability to encapsulate, stabilize and subsequently release a commercial biocide used for latex preservation (CMIT/MIT). CMIT/MIT consists of an aqueous solution of the active ingredients CMIT (5-chloro-2-methyl-4-isothiazolin-3-one) and MIT (2-methyl-4-isothiazolin-3-one), present in a CMIT/MIT: 3/1 wt ratio. It was observed that the biocide can be encapsulated in both silica frameworks without suffering structural damage. The SBA-15 support exhibits a lower adsorption capacity of biocide molecules than MCF, which may be attributed to both agreater MCF pore volume and pore size. MCF has less hindered diffusion causedby a short channel length, which facilitates the biocide access to the pores ofthe matrix. The long pore length of SBA-15 makes the diffusion of CMIT/MIT mixture more difficult. Biocide release tests in aqueous media indicated that the CMIT/MIT concentration in the leaching solution depends on the matrix nature, the smaller values being obtained when the ordered matrix was used. Additionally, biocide delivery could be delayed by increasing the working pH from 7 to 9. Results showed that biocide encapsulation allows maintaining a long-lasting release, even under alkaline conditions (pH 9), at which the hydrolysis of non-supported CMIT occur. Several release tests at different temperature (318, 323 and 328 K), were carried out for 20 days at pH 7. The biocide loading after the tests was reflected in the IR spectra, and it has been corroborated that biocide encapsulation allows retarding the fast thermal decomposition of CMIT.

1. Introduction

Isothiazolinones are a class of broad spectrum biocides used to control the growth of microorganisms such as bacteria, fungi and yeast, and are generally employed for preserving different industrial formulations. Compared to other biocides, isothiazolinones are very effective, fast-acting compounds for the inhibition of microbial growth and metabolism, aside from being capable of controlling biofilm development. These biocides are frequently used for the control of microbial growth in different industrial arrangements, such as cooling water systems, industrial water treatment, oil extraction systems, fuel storage tanks, pulp and paper mills, wood preservation, antifouling agents, coating industry, personal-care and cosmetic industry, etc. [1–3].

In the coating industry, isothiazolinones are included in waterborne formulations such as paints for walls, printing inks, adhesives, and sealants [4]. At first, during the manufacturing process, a fast biocide action is necessary to reduce the great amount of microorganisms present in the raw materials and industrial water. Then, in the storage and transport stage, the biocide action must continue because the acidic metabolic products of the remaining microorganisms could reduce the pH, destabilizing the film-forming material emulsion. This fact causes, in turn, different drawbacks, mainly malfunction of additives, odor generation and poor film adhesion.

The commercial formulation most frequently used in the coating industry for providing wet state protection is a 1.5 wt% aqueous solution containing both 5-chloro-2-methyl-4-isothiazolin-3-one (CMIT) and 2-methyl-4-isothiazolin-3-one (MIT) in a CMIT/MIT = 3 wt ratio [5]. The MIT and CMIT structure is shown in Fig. 1.

The mechanism proposed for CMIT/MIT is based on its electrophilic characteristics, which allow it to react with critical enzymes, inhibiting growth and metabolism, leading to irreversible cell damage occurring

* Corresponding author.
E-mail address: eib@quimica.unlp.edu.ar (E.I. Basaldella).

https://doi.org/10.1016/j.porgcoat.2018.02.023
Received 14 July 2017; Received in revised form 31 January 2018; Accepted 21 February 2018

Nomenclature

C_e	Equilibrium liquid phase concentration (mg/mL)	1/n	Freundlich constant
C_0	Initial biocide concentration (mg/mL)	q_e	Equilibrium solid phase concentration (mg/g)
ΔG°ads	Gibbs free energy of adsorption (kJ/mol)	*R*	Universal gas constant (8.314 J/(mol K))
ΔH°ads	Enthalpy of adsorption (kJ/mol)	R^2	Regression correlation coefficient
Kc	Equilibrium constant for the adsorption process	ΔS°_{ads}	Entropy of adsorption (J/mol K)
k_F	Freundlich constant, (mg/g (mL/mg)$^{1/n}$	*T*	Temperature (K)
		T	Time (h)
		V	Volume of solution (mL)

after several hours. Therefore, CMIT/MIT is effective against aerobic and anaerobic microorganisms because the key enzymes involved in the inhibition process are present in both species [6].

Despite its effectiveness as a successful preservative, CMIT/MIT is a strong sensitizer, producing skin irritation and allergies [7–9], and could pose ecotoxicological risks [1]. Consequently, its use has been restricted by EU legislation to limited concentrations depending on the product type to be preserved [10,11].

This preservative generally displays excellent performance, but its effectiveness has to be checked when it is included in a particular product. Incompatibilities between constituents, thermal sensitivity above 313 K, and instability in strong alkaline media (pH ≥ 8) would be the reasons for the decrease of its preservative properties [12].

In addition, during the storage and transport steps, the paint could be subjected to high temperatures, leading to the biocide decomposition and consequently to the loss of its killing power. Without biocide in the wet state of paint, the bacteria degrade organic materials (polymer and cellulosic additives act as nutrients) generating gases (hydrogen chloride, nitrogen oxides, sulfur oxides) that could cause rapid pressure buildup in closed systems or cans. Then, maintaining the biocide release beyond 313 K is an additional challenge. Kazeminski et al. [12,13], monitored the aqueous degradation of isothiazolinones as a function of temperature and pH. They found that the half-life for the first-order decomposition of isothiazolinones was 4.6 days at 313 K and 0.48 days at 333 K. As a function of pH, at 297 K the half-lives were 46 days at pH = 8.5, and 3.41 days at pH = 9.62.

Recent studies about biocide encapsulations by adsorption onto nanoporous inorganic materials indicate that this procedure could be appropriate for obtaining a longer-term protection from microbiological attack [14–16]. The supported biocide could be slowly released because adsorption interactions between the adsorbate molecules and the inorganic framework render the biocide more resistant to leaching [17–20]. In this way, biocide encapsulation could be an environmentally friendly option because the incorporation of high initial biocide concentrations to ensure long-term preservation would be avoided [14–22].

Mesoporous silica nanocarriers can offer many advantages as vehicles for controlled release, such as high surface area, well-defined and tunable pore size. The most often used mesoporous silica-based vehicles have been the SBA series [23–25]. In particular, SBA-15 is a mesoporous material presenting unidirectional cylindrical pores and pore volume of about 1 g/cm^3. These properties favor adsorption processes and the development of slow release formulations [26–31]. On the other hand, mesocellular siliceous foam (MCF) is a mesoporous material that consists of uniform cells and windows [32]. The uniform windows interconnect the spherical cells forming a continuous three-dimensional (3D) pore system [33]. It is known that the particle size and morphology of the siliceous matrices, as well as the size, volume and geometry of the pores, are all important parameters determining the release rate of the incorporated molecules [34,35].

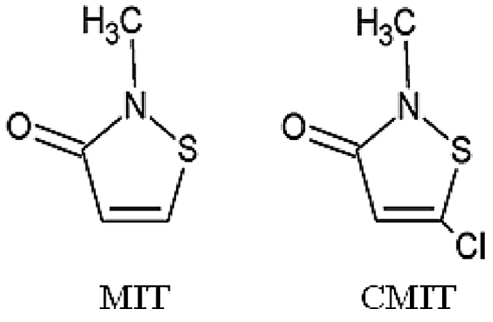

Fig. 1. Methylisothiazolinone (MIT) and chloromethylisothiazolinone. Chloromethylisothiazolinone (CMIT) structure.

In the search for an enhancement of CMIT/MIT stability, in this paper the biocide encapsulation in mesoporous materials SBA-15 and MCF synthesized at our laboratory is proposed. The improvement of the biocide stability was analyzed in terms of obtaining a delayed biocide degradation, minimizing the disadvantages associated with hydrolysis at high pH values and decomposition at temperatures above 313 K.

2. Experimental

2.1. Chemicals

The chemicals used in this study include triblock copolymer poly (ethylene oxide)-poly(propylene oxide)-poly(ethyleneoxide) (Pluronic P123, MW: 5800, Aldrich), tetraethyl orthosilicate (TEOS, 98%, Aldrich), hydrochloric acid (HCl, 37%, Anedra), mesitylene (MES, 98%, Aldrich) and a commercial aqueous biocide for latex preservation composed of a mixture of 5-chloro-2-methyl-2H-isothiazol-3-one and 2-methyl-2H-isothiazol-3-one (Rohm and Haas).

2.2. Synthesis of materials

SBA-15 mesoporous silica was prepared according to the methodology described by Zhao [36]. In a typical preparation, 4 g of Pluronic P123 block copolymer was dissolved in 4 mL of 2 M HCl aqueous solution under stirring at 35 °C. Then, 8 g of TEOS was added dropwise to the mixture, under stirring. The stirring was continued for 20 h. Subsequently, the reacting mixture was heated to 80 °C for 24 h. The molar composition used was 1TEOS:5HCl:0.018PEO:184H_2O. The solid material obtained was washed with water, dried at 120 °C, and calcined for 6 h at 540 °C. MCF was obtained employing a procedure similar to that previously described for obtaining the SBA-15, differing in the addition of mesitylene to the synthesis mixture [33]. The molar composition of the gel was 1TEOS:1.15MES:5HCl:0.018PEO:184H_2O.

2.3. Characterization

In order to determine the morphology and particle size of the materials, a Philips 505 scanning electron microscope (SEM) was used. Transmission electron microscopy (TEM) was performed with a JEOL100CX instrument operated at 100 kV. For the preparation of SEM samples, a small amount of sample was placed on carbon tape and sputter coated with gold. For the preparation of TEM samples, a small amount of the sample was suspended in hexane before being deposited on specific grids (400 mesh copper grid covered with an ultrathin carbon membrane of 2–3 nm thickness).

The X-ray diffraction (XRD) measurements were carried out on a

Rigaku Ultima IV diffractometer using CuKα radiation, with a scan speed of 0.2°/min at 40 kV and 44 mA, and a step size of 0.02° (2θ).

The adsorption-desorption nitrogen isotherms were determined in Micromeritics ASAP 2020 apparatus at the temperature of liquid nitrogen (−196 °C) using a relative pressure range 0.01–0.99. Before adsorption, samples were out-gassed by heating at 100 °C in vacuum, with a pressure lower than 3×10^{-2} mm Hg for 12 h. The Brunauer–Emmett–Teller (BET) equation was used to calculate the surface area [37]. The pore size distributions (PSD) of the solids were obtained by the VBS macroscopic method [38] using the adsorption branch data. The pore volume was taken at $P/P_0 = 0.989$.

Shimadzu IRAffinity-1 Fourier transform infrared equipment, pellets in KBr, and a measuring range of 400–4000 cm^{-1} were used to obtain the FT-IR spectra. The samples were placed directly into the chamber, and 48 scans were used for each spectrum.

2.4. Biocide load measurements

To evaluate the adsorption capacity of the materials, the SBA-15 and MCF samples were soaked in a solution of biocide in water (concentration 150 mg/mL). It was proved that isothiazolinones are highly soluble in water, preserving their structure in aqueous media. This was the main reason for using water, the cheapest solvent, to prepare the loading solutions. The resulting suspensions (20 mg solid/mL liquid) were left at ambient temperature, with stirring, for 6 h. The solid phases were separated from the liquids by filtration and dried at room temperature. The samples were named SBA15/bio and MCF/bio.

For the adsorption isotherm experiments, batch solutions of 100 mL with concentrations ranging from 10 to 30 mg/mL of biocide were mixed with 1 g of adsorbent and shaken for 6 h at room temperature.

In all cases, the equilibrium concentration of each solution was determined by UV–vis spectroscopy at 274 nm (UV-1800 Shimadzu, Japan).

2.5. In vitro biocide release

In order to determine the pH influence on the degradation of CMIT/MIT when it was loaded into the matrices, release studies were carried out by adding 0.2 g of the corresponding biocide-loaded sample (SBA15/bio and MCF/bio) to 100 mL of a pH controlled aqueous solution, at room temperature and under stirring. Aqueous solutions at pH values of 8.0, 8.5 and 9.0 were used. The pH values were adjusted by adding an appropriate volume of a 0.1 N NaOH solution. The working pH values were selected based on the fact that at present, in attempts to improve rheological properties, some coatings are formulated at pH higher than 8, probably inducing the hydrolysis of CMIT. Besides, the assays were performed up to 14 days, preventing the occurrence of CIM hydrolysis [39]. Aliquots of 3 mL were removed from the mixture at regular time intervals and replaced with fresh medium in order to maintain sink conditions. The concentration of the biocide in the liquid phase was determined using UV–vis spectroscopy. A release test at pH = 7 was carried out as reference. A release test under very aggressive conditions (pH = 9 and T = 328 K, under stirring) was also performed. Additionally, the presence of remaining CMIT molecules after 20 days of release at 318, 323 and 328 K, at pH 7, was checked by FTIR.

3. Results and discussion

3.1. Adsorbent characterization

SEM images of SBA-15 and MCF materials are shown in Fig. 2. The SEM image showed that the SBA-15 sample consisted of rod-like subparticles of relatively uniform size, 1 μm in diameter and 14–16 μm in length (Fig. 2a). On the other hand, a change in the morphology of the particles was attained by adding mesitylene to the synthesis mixture. The MCF sample exhibited spherical aggregates consisting of rounded particles about 4–6 μm in size (Fig. 2b).

TEM images confirmed the two-dimensional hexagonal structure (p6 mm) of SBA-15-type materials and showed an ordered arrangement

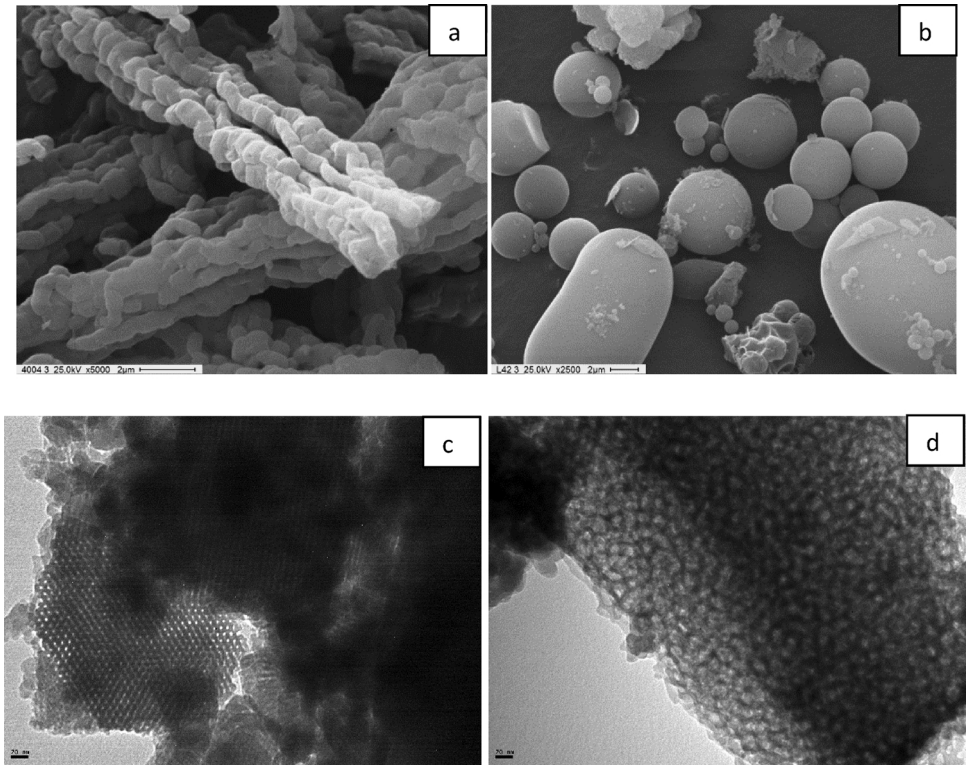

Fig. 2. SEM images of SBA-15 (a) and MCF (b). TEM Images of SBA-15 (c) and MCF (d).

of cylindrical pores (Fig. 2c). In the case of MCF, the structural regularity was completely lost. TEM images show interconnected disordered oval-shaped pores (Fig. 2d).

The X-ray diffraction results were consistent with the TEM images. The powder X-ray diffraction patterns of both mesoporous silicas are shown in Fig. 3. Sample SBA-15 clearly displays the characteristic d_{100} peak of SBA-15 structure at a 2θ value of about 0.98° and two smaller reflections corresponding to d_{110} and d_{200}, in agreement with the original report [36].

In sample MCF, there is a peak at a 2θ value of 0.76° indicating the existence of the ultralarge mesopores. The increase in pore diameter shifts the position of the (100) plane to *2θ* lower values.

Adsorption and desorption isotherms of N_2 on the silica materials are shown in Fig. 4. All the studied samples exhibit Type IV isotherms according to the IUPAC classification. The SBA-15 sample shows a type H1 hysteresis loop, which is associated with mesoporous materials consisting of well-defined cylindrical-like pore channels. [40]. Fig. 5 shows the mesopore size distribution curve calculated by applying the VBS macroscopic method. A narrow pore size distribution with a mean value of 6.1 nm is obtained from the desorption branch of the isotherm. The BET surface area of SBA-15 is 578 m^2/g with a total pore volume of 0.48 cm^3/g.

A very sharp desorption branch was recorded for MCF. Hysteresis loops of this type are given by more complex pore structures in which network effects are important. The very steep desorption branch observed can be attributed either to pore-blocking/percolation in a narrow range of pore necks or to cavitation-induced evaporation [41].

The textural characteristics of the synthesized solids are summarized in Table 1. It could be noted that after biocide adsorption on both SBA-15 and MCF, a significant reduction in the surface area, pore volume and pore size occurred.

3.2. Adsorption equilibrium of MIT/CMIT on mesoporous materials

The successful loading of biocide in mesoporous silica materials was evidenced by the distinct decreased of pore diameters, pore volumes, and BET surface areas after the MIT/CMIT mixture adsorption. The percentage of biocide adsorbed for SBA-15 and MCF is shown in Table 1.

The SBA-15 support exhibits a lower adsorption capacity of biocide molecules than MCF, which may be attributed to both higher MCF pore volume and pore size (Table 1). In addition, MCF has less hindered diffusion caused by a short channel length, which facilitates the access of the biocide into the pores of the matrix. The long pore length of SBA-15 makes the diffusion of CMIT/MIT mixture more difficult. It is possible that the entrance of guest molecules to a determined level of pore channels obstructs the subsequent adsorption. The results show that the morphologies and pore sizes of mesoporous silica affect the loading of guest molecules, which is consistent with our previous work [42,43].

The adsorption equilibrium isotherm is based on the mathematical relationship between the adsorbed amount per gram of adsorbent (q_e) and the equilibrium solution concentration (C_e) at a fixed temperature [44]. In this study the Langmuir and Freundlich isotherms in their linear forms were applied to the equilibrium data of adsorption of MIT/CMIT on SBA-15 and MCF (Table 2).

The Langmuir isotherm is valid for the monolayer adsorption of solute from liquid solution and there was no interaction between the adsorbed ions. It describes the adsorption onto the surface through uniform energy, and no adsorption in the surface plane of the transmigration. Langmuir adsorption depends on the assumption that the intermolecular forces decrease rapidly with distance. Adsorption takes place at specific homogeneous sites within the adsorbent [45]. Conversely, the Freundlich equilibrium isotherm equation is an empirical equation used for the description of multilayer adsorption with interaction between adsorbed molecules. The model is applicable to the adsorption on heterogeneous surfaces by a uniform energy distribution and reversible adsorption. The applicability of the Freundlich adsorption isotherm was assessed by plotting ln q_e versus ln C_e. The magnitude of the exponent 1/n gives an indication of the intensity of the adsorption or surface heterogeneity, becoming more heterogeneous as its value gets closer to zero. If $1/n < 1$, adsorption is a favorable physical process [46].

3.3. Temperature effect on the CMIT/MIT adsorption capacity of mesoporous materials

Fig. 6 show the adsorption isotherms of biocide according to the Freundlich model. The isotherm constants and correlation coefficients obtained for the isotherm models are summarized in Table 3. Freundlich model gave the highest R^2 values for the two adsorbents. Therefore, this model is the best one to describe the data. The 1/n values are lower than 1.0, suggesting that biocide is favorably adsorbed by the two adsorbents and conducted by van der Waals forces [47].

The Gibbs free energy change ΔG° indicates the degree of spontaneity of the adsorption process. For significant adsorption to occur, the free energy changes of adsorption, ΔG°, must be negative. The Gibbs free energy change of the adsorption process was calculated by using the following equations:

$$-\Delta G^{\circ}ads = -RT \ln K_C$$

The equilibrium constant for the adsorption process, K_C (1) [48], was evaluated at 298, 308 and 318 K (Table 4) and calculated with the following equation:

$$1\ K_C = Ce/(C_0 - Ce)$$

The effect of temperature on the equilibrium constant is determined as follows:

$$\ln Kc = \Delta S^{\circ}ads/R - \Delta H^{\circ}ads/RT$$

The values of the slope $-\Delta H^{\circ}ads/R$ and the intercept $\Delta S^{\circ}ads/R$ from Fig. 7 give standard enthalpy (ΔH°ads) and entropy (ΔS°ads) for the adsorption of CMIT/MIT on the mesoporous silicas. The values of the thermodynamic parameters (ΔG°ads, ΔH°ads and ΔS°ads) are listed in Table 4.

The negative value of the free energy change (ΔG°) confirms the feasibility of the adsorption process and also indicates spontaneous adsorption of CMIT/MIT onto SBA-15 and MCF in the temperature range studied. In all cases, the small positive values of the standard enthalpy change (ΔH°) indicate that the adsorption is physical in nature involving weak forces of attraction and is also an endothermic process. The positive values of ΔS°ads show an irregular increase of the randomness at the composite-solution interface during adsorption.

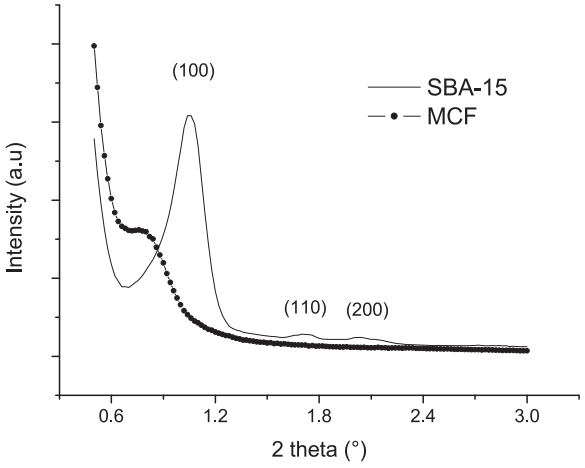

Fig. 3. XRD patterns of SBA-15 and MCF.

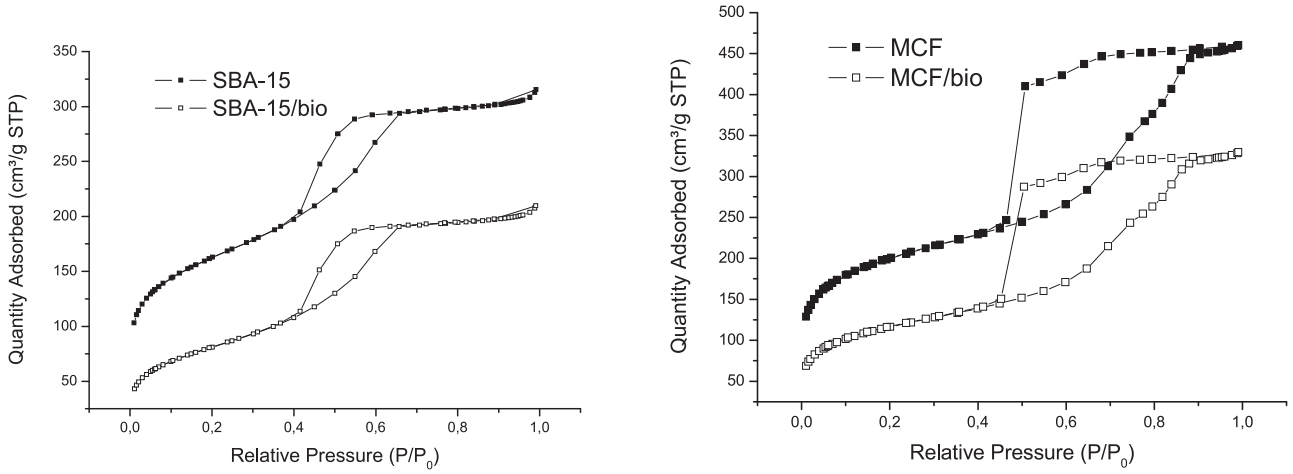

Fig. 4. Nitrogen adsorption/desorption isotherms of SBA-15 and MCF before and after biocide adsorption.

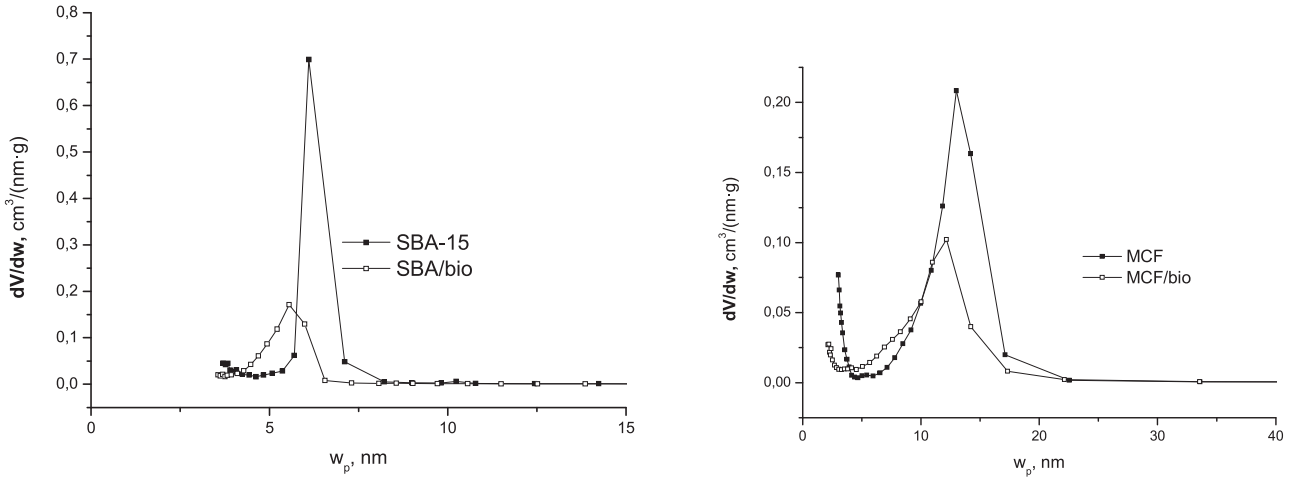

Fig. 5. Pore size distribution of SBA-15 and MCF before and after biocide adsorption.

Table 1
Textural properties of SBA-15 and MCF before and after biocide adsorption.

Sample	S BET (m^2/g)	Pore vol. (cm^3/g)	Pore size (nm)	% loaded
SBA-15	578 +/− 2	0.48	6.1	–
MCF	713 +/− 3	0.71	13	–
SBA-15/bio	247 +/− 2	0.34	5.5	18
MCF/bio	261 +/− 2	0.63	12.1	27

Table 2
Linear forms of the Langmuir and Freundlich adsorption isotherms used in this study.

Models	Equations	Parameters	References
Freundlich	$ln\ q_e = ln K_f + 1/n\ ln\ C_e$	K_f, $1/n$	46

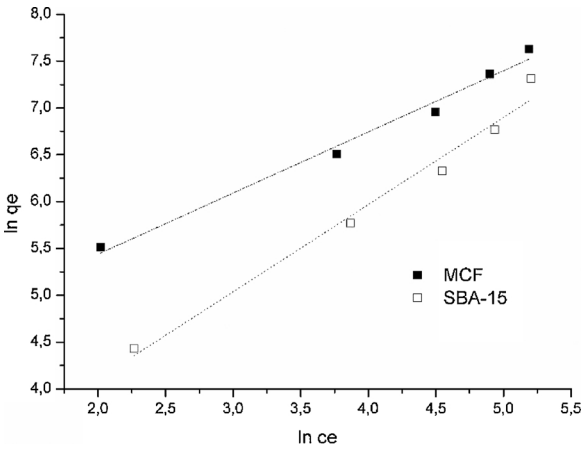

Fig. 6. Equilibrium adsorption isotherms of MIT/CMIT on SBA-15 and MCF fitted to Freundlich model.

3.4. Biocide release study

The release profiles of CMIT/MIT from SBA15/bio and MCF/bio at different pH values were determined at room temperature. The influence of pH and the behavior according to the material type can clearly be observed in Fig. 8.

As is shown in Fig. 8, the release rate for both materials exhibits two steps; the first one is a fast delivery followed by a second stage where there is a slower rate of delivery.

It is also observed that the CMIT/MIT concentration in the leaching solution depends on the matrix type. MCF/bio showed a fast CMIT/MIT release of 21–32 wt% only at 3 h for the fast delivery step (Fig. 8a) but with residual activity since the biocide delivery percentage attained 55–65 wt% at 14 days, depending on the working pH (Fig. 8b). Compared to MCF, SBA-15 structure showed a slower release rate both short and long release times (20–24%wt at 3 h for the fast delivery step, reaching 42–52 wt% at 14 days, Fig. 8c and d respectively). These

Table 3
Parameters of the isotherm models.

Adsorbents	Freundlich		
	K_f (mg/g(L/mg)$^{1/n}$)	1/n	R^2
SBA-15	9.45	0.93	0.9818
MCF	62.33	0.65	0.9873

Table 4
Thermodynamic parameters for the adsorption of MIT/CMIT on SBA-15 and MCF silicas.

Sample	T	SBA-15	MCF
Kc	298	5.76	2.07
	308	8.45	2.32
	318	11.01	2.9
−ΔG°ads (KJ/mol)	298	4.34	1.8
	308	5.46	2.16
	318	6.02	2.67
ΔH°ads (KJ/mol)		25.6	13.2
ΔS°ads (J/mol K)		100.56	50.3
R^2		0.9925	0.9627

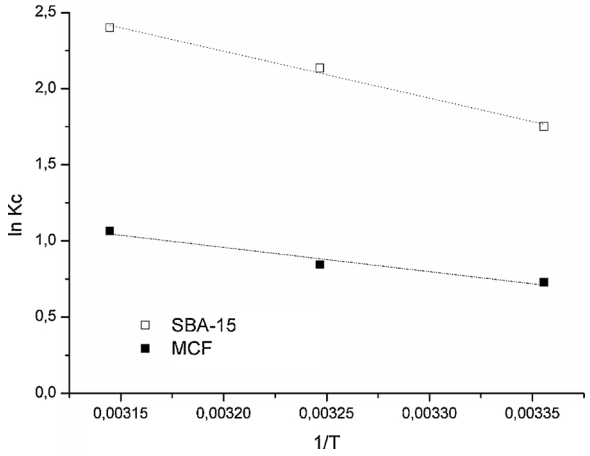

Fig. 7. Plot of ln K_C as a function of the reciprocal of temperature (1/T) for the adsorption of CMIT/MIT on SBA-15 and MCF silicas.

results suggest that these materials canbe used as potential hosts for paint formulations. Then MCF/bio would be helpful in the first step of coating manufacture, where rapid removal of microorganisms is required, and SBA-15/bio could be useful for controlled delivery over long periods, i.e., in the product transport or storage stages. Then, the textural properties, surface geometry and bulk porosity of siliceous matrices are factors affecting or controlling the release of the biocide. The release of CMIT/MIT from MCF/bio was higher compared to that of SBA-15/bio, due to the pore characteristics of MCF structure. The slight narrowing of SBA-15 pores could significantly retard the biocide delivery and also decreases the amount released. Regarding the influence of particle size, it is supposed that pore lengths generally present in these solids could be reduced when smaller sized particles are used. Nevertheless, the pore shape and morphology of SBA-15 and MCF are too different to establish a comparison in terms of particle size. For determining the influence of the matrix particle size, it was necessary to use particles presenting the same kind of mesoporous structure but differing in size. We have done previous studies about this subject that are detailed in ref. [43].

Regarding the pH influence, from the analysis of the curves presented in Fig. 8, it is also noted that for short times of delivery (24 h, Fig. 8a), CMIT/MIT release from MCF/bio reached 45 wt% at pH = 7, 39 wt% at pH = 8, 35 wt% at pH = 8.5, and 34 wt% at pH = 9. At 14 days of the test, the CMIT/MIT release values reached 65, 62, 59, 54 wt% for increasing pH values, respectively. For SBA-15/bio (Fig. 8c) at 24 h of the test, the CMIT/MIT percentages released were 36 wt% at pH = 7, 31 wt% at pH = 8, 28 wt% at pH = 8.5, and 27 wt% at pH = 9. At the end of the test (14 days, Fig. 8d), the CMIT/MIT release for increasing pH values was 52, 49, 44 and 42 wt%. Therefore, it is clearly seen that the two siliceous materials are capable of releasing the biocide preferentially at lower pH of the medium. The retarded release observed as the pH increased could be explained on the basis of strong CMIT/MIT-mesoporous solid interactions as a result of van der Waals forces and electrostatic interactions. Taking into account that the point of zero charge of both matrices is evidenced at very low pH values (which is about 4.3 [49]), the higher pH values of the leaching solution would favor a balance of negative charges on the surface of siliceous materials. Then, as the alkalinity of the medium increases, there would be a greater availability of silanol groups that can interact with the positive ring and methyl group of both biocide molecules (CMIT and MIT). The ring and methyl group of the biocide contribute to stabilizing the negative charge of the silica surface [43].

Fig. 9 shows the infrared spectra of SBA15/bio and MCF/bio at 318, 323 and 328 K after 20 days of the release test at pH = 7. For the two samples, regardless of the temperature used, asymmetric stretching vibrations of Si—O—Si at 1100 cm^{-1}, symmetric stretching vibrations from Si—O bonds at 800 cm^{-1}, and bending vibrations from Si—O—Si at 456 cm^{-1} are clearly observed. The peaks around 960 cm^{-1} correspond to noncondensed Si OH groups [50,51]. The broad band around 3400 cm^{-1} and the strong peak around 1630 cm^{-1} are due to the stretching and bending vibrations of adsorbed H_2O.

The biocide loading was reflected in the IR spectra by the presence of the stretching vibration bands of C—H at 2940, 2890 and 886 cm^{-1}, and bending vibration bands of C—H observed in the range 1450–1390 cm^{-1}. The band around 600 cm^{-1} is due to C—Cl stretching [52].

Fig. 9 corroborated the presence of biocide in SBA-15 and MCF. In all cases, the shoulder around 670 cm^{-1} corresponding to C—Cl stretching appears in the FTIR spectra. This fact confirms the presence of CMIT in the siliceous material still at temperatures higher than the ones corresponding to its thermal decomposition. Then, biocide encapsulation allows retarding the fast thermal decomposition above 313.

On the other hand, the shoulder around 670 cm^{-1} corresponding to C—Cl stretching also appears after 20 days of the release test at pH = 9 for both siliceous materials in FTIR analysis (Fig. 10). This fact confirms the presence of CMIT in the SBA-15 and MCF beyond 14 days (time suggested for CMIT hydrolysis to occur) [39]. It was also noted that very aggressive test conditions (pH = 9 and T = 328 K) caused difficulties in the control of CMIT/MIT release for the two materials. The release rate began to accelerate from 12 days because of the structural matrix degradation and, as expected, the percentage of release immediately reached 100% (not shown). Clearly, the structured matrices began to lose mass up to their completely destruction.

4. Conclusions

Isothiazolinone adsorption on the different siliceous matrices led to a decrease in surface area and pore volume, indicating biocide adsorption inside the mesopores. Additionally, the biocide original structure was always preserved after the adsorption test.

Release tests in aqueous media indicated that the CMIT/MIT concentration in the leaching solution depends on the structural arrangement of siliceous material, the higher values being obtained when disordered matrices were used. Silicas presenting structural disordering seem to be the most effective matrices for fast release, whereas ordered matrices are more suitable for biocide encapsulation.

The stability of supported biocide in strong alkaline media and its sensitivity to temperatures higher than 313 K were also studied. Results indicated that higher pH values of test solutions slightly delayed the

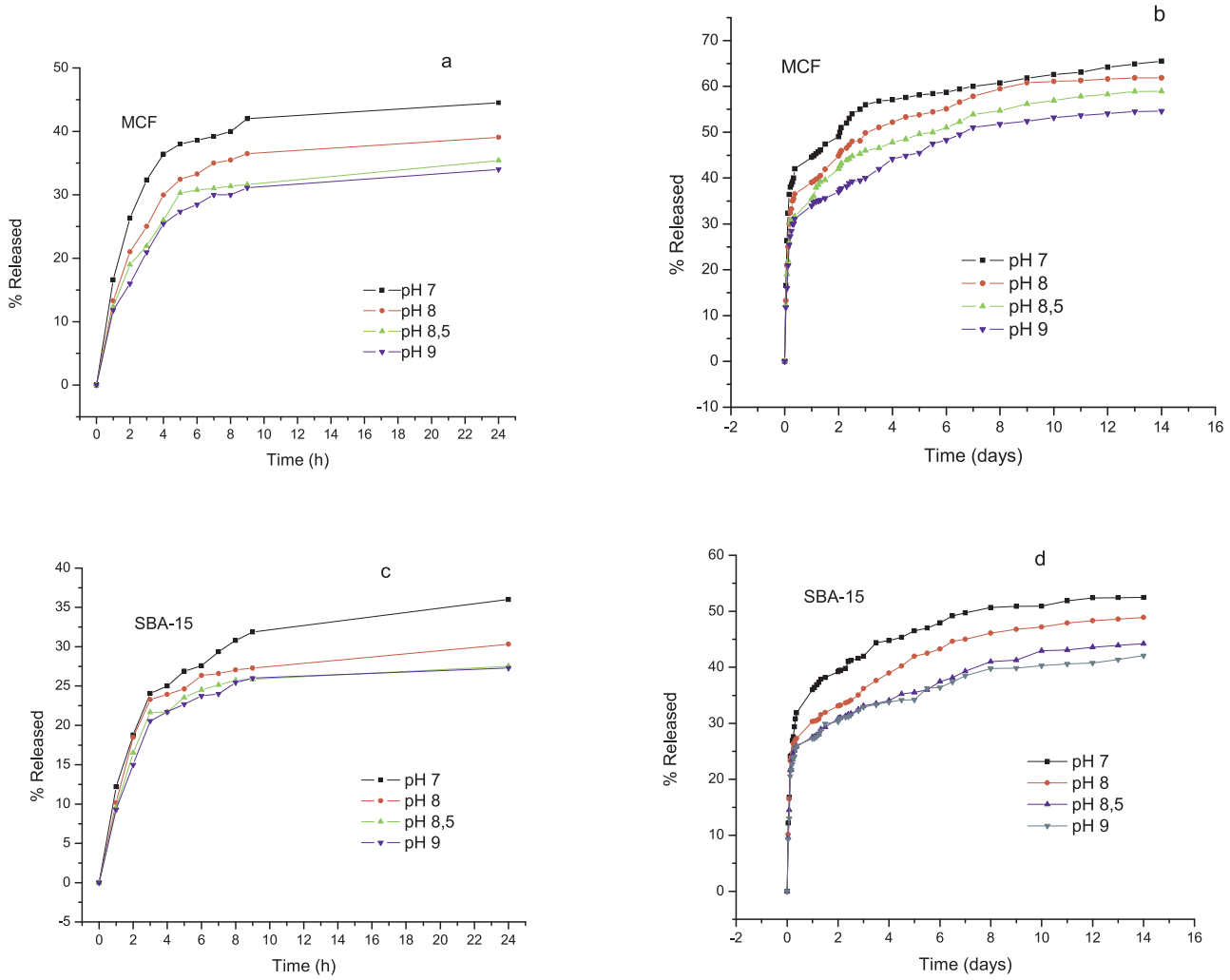

Fig. 8. Release experiments from SBA15/bio and MCF/bio.

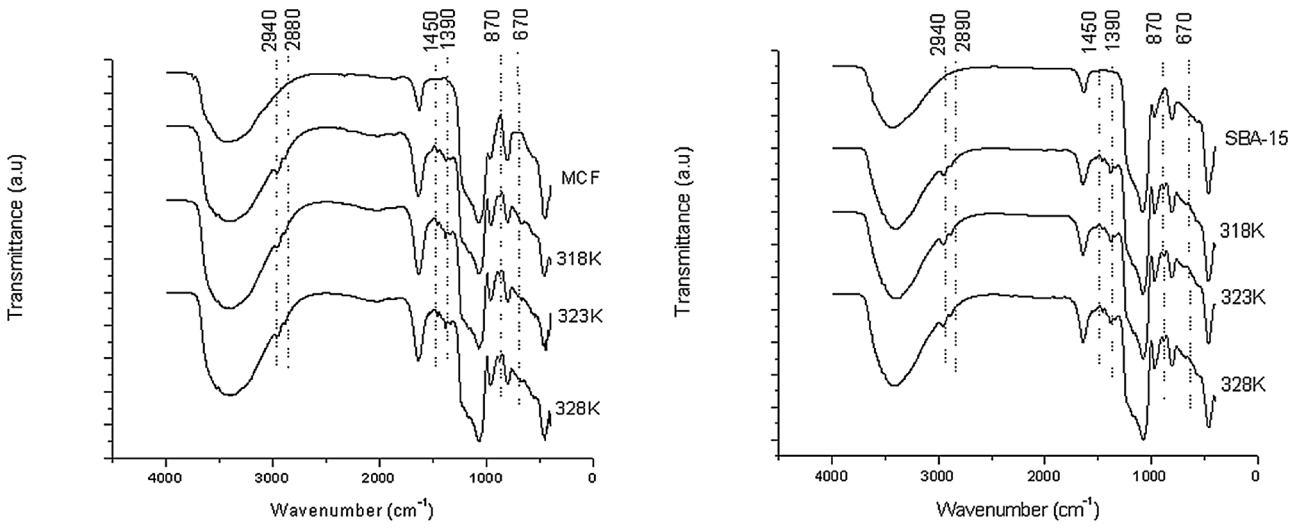

Fig. 9. FTIR analysis of loaded SBA-15 and MCF after 20 days of the release test at 318, 323 and 328 K (pH 7).

biocide delivery. Additionally, the test up to 328 K corroborated that biocide encapsulation allowed retarding the fast thermal decomposition of CMIT.

Results showed that the incorporation of CMIT/MIT into inert matrices could be advantageous because the biocide encapsulation would allow maintaining a permanent release, preserving its biocidal activity even under conditions of temperature and pH at which the decomposition and hydrolysis of CMIT occur. The results provide some evidence that the biocidal compound could be released reducing environmental and human risks, improving the quality of the products.

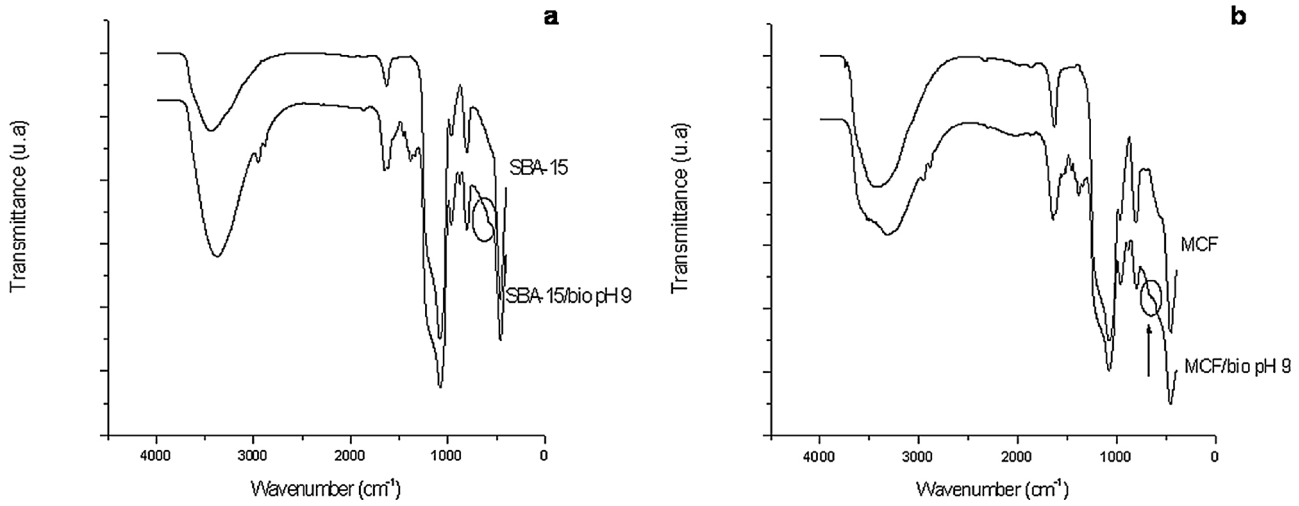

Fig. 10. FTIR analysis of loaded SBA-15 and MCF after 20 days of the release test at pH 9 and room temperature.

Acknowledgments

The authors would thank CIC-PBA, FONCyT (Project PICT 2012-2421), UTN, UNLP and CONICET for their financial support. E.I. Basaldella is a member of CIC-PBA.

References

[1] A. Rafoth, S. Gabriel, F. Sacher, H. Brauch, Analysis of isothiazolinones in environmental waters by gas chromatography–mass spectrometry, J. Chromatogr. A 1164 (2007) 74–81.
[2] G. Alvarez-Rivera, T. Dagnac, M. Lores, C. Garcia-Jares, L. Sanchez-Prado, J. Lamas, M. Llompart, Determination of isothiazolinone preservatives in cosmetics and household products by matrix solid-phase dispersion followed by high-performance liquid chromatography–tandem mass spectrometry, J. Chromatogr. A 1270 (2012) 41–50.
[3] M. Moradi, J. Duan, X. Du, Investigation of the effect of 4,5-dichloro-2-n-octyl-4-isothiazolin-3-one inhibition on the corrosion of carbon steel in Bacillus sp. inoculated artificial seawater, Corros. Sci. 69 (2013) 338–345.
[4] R. Nagorka, C. Gleue, C. Scheller, H. Moriske, W. Straff, Isothiazolone emissions from building products, Indoor Air 25 (2015) 68–78.
[5] N. Hunziker, The isothiazolinone story, Dermatology 184 (1992) 85–86.
[6] T. Williams, The mechanism of action of isothiazolinones, PowerPlant Chem. 9 (2007) 14–22.
[7] M. Tokunaga, H. Fujii, K. Okada, Y. Kagemoto, T. Nomura, M. Tanioka, Y. Matsumura, Y. Miyachi, Occupational airborne contact dermatitis by isothiazolinones contained in wall paint products, Allergol. Int. 62 (2013) 395–397.
[8] A. De Groot, A. Herxheimer, Isothiazolinone preservative: cause of a continuing epidemic of cosmetic dermatitis, Lancet 333 (1989) 314–316.
[9] J. Garcia-Gavin, S. Vansina, S. Kerre, A. Naert, A. Goossens, Methylisothiazolinone, an emerging allergen in cosmetics? Contact Dermatitis 63 (2010) 96–101.
[10] Cosmetics: regulation (EC) No. 1223/2009 of the european parliament and of the council of 30 November 2009 on cosmetic products (recast), Off. J. Eur. Union L342 (2009) 59.
[11] G. Davison, B. Lane, Paints Additives in Water-borne Coatings, The Royal Society of Chemistry, London, 2003.
[12] S.F. Kazeminski, C.K. Brackett, J.D. Fisher, Fate of microbicidal 3-isothiazolone compounds in the environment: modes and rates of dissipation, J. Agric. Food Chem. 23 (1975) 1060–1068.
[13] S.F. Kazeminski, C.K. Brackett, J.D. Fisher, J.F. Spinnler, Fate of microbicidal 3-isothiazolone compounds in the environment: products of degradation, J. Agric. Food Chem. 23 (1975) 1068–1075.
[14] G. Sørensen, A.L. Nielsen, M.M. Pedersen, S. Poulsen, H. Nissen, M. Poulsen, S.D. Nygaard, Controlled release of biocide from silica microparticles in wood paint, Prog. Org. Coat. 68 (2010) 299–306.
[15] J. Eversdijk, S.J.F. Erich, S.P.M. Hermanns, O.C.G. Adan, M. De Bolle, K. de Meyer, D. Bylemans, M. Bekker, A.T. ten Cate, Development and evaluation of a biocide release system for prolonged antifungal activity in finishing materials, Prog. Org. Coat. 74 (2012) 640–644.
[16] J. Bergek, M. Andersson Trojer, A. Mok, L. Nordstierna, Controlled release of microencapsulated 2-n-octyl-4-isothiazolin-3-one from coatings: effect of microscopic and macroscopic pores, Colloids Surf. A: Physicochem. Eng. Asp. 458 (2014) 155–167.
[17] Y. Liu, P. Laks, P. Heiden, Controlled release of biocides in solid wood. II. Efficacy against *Trametes versicolor* and *Gloeophyllum trabeum* wood decay fungi, J. Appl. Polym. Sci. 86 (2002) 608–614.
[18] Y. Liu, L. Yan, P. Heiden, P. Laks, Use of nanoparticles for controlled release of biocides in solid wood, J. Appl. Polym. Sci. 79 (2001) 458–465.
[19] Y. Liu, P. Laks, P. Heiden, Controlled release of biocides in solid wood. III. Preparation and characterization of surfactant-free nanoparticles, J. Appl. Polym. Sci. 86 (2002) 615–621.
[20] S. Jämsä, R. Mahlberg, U. Holopainen, J. Ropponen, A. Savolainen, A.-C. Ritschkoff, Slow release of a biocidal agent from polymeric microcapsules for preventing biodeteroration, Prog. Org. Coat. 76 (2013) 269–276.
[21] M.A. Shirakawa, R. Gonçalves Tavares, C.C. Gaylarde, M.E. Santos Taqueda, K. Loh, V.M. John, Climate as the most important factor determining anti-fungal biocide performance in paint films, Sci. Total Environ. 408 (2010) 5878–5886.
[22] S. Coutu, C. Rota, L. Rossi, D.A. Barry, Modelling city-scale facade leaching of biocide by rainfall, Water Res. 46 (2012) 3525–3534.
[23] M. Moritz, M. Łaniecki, SBA-15 mesoporous material modified with APTES as the carrier for 2-(3-benzoylphenyl)propionic acid, Appl. Surf. Sci. 258 (2012) 7523–7529.
[24] Y. Ding, G. Yin, X. Liao, Z. Huang, X. Chen, Y. Yao, J. Li, A convenient route to synthesize SBA-15 rods with tunable pore length for lysozyme adsorption, Microporous Mesoporous Mater. 170 (2013) 45–51.
[25] É. Pérez-Esteve, M. Ruiz-Rico, C. de la Torre, L.A. Villaescusa, F. Sancenón, M.D. Marcos, P. Amorós, R. Martínez-Máñez, J. Barat, Encapsulation of folic acid in different silica porous supports: a comparative study, Food Chem. 196 (2016) 66–75.
[26] S. Park, P. Pendleton, Mesoporous silica SBA-15 for natural antimicrobial delivery, Powder Technol. 223 (2012) 77–82.
[27] Y. Xu, C. Wang, G. Zhou, Y. Wu, J. Chen, Improving the Controlled release of water-insoluble emodin from amino-functionalized mesoporous silica, Appl. Surf. Sci. 258 (2012) 6366–6372.
[28] M.S. Legnoverde, I. Jiménez-Morales, E. Rodríguez-Castellón, A. Jiménez-Morales, E.I. Basaldella, Modified silica matrices for controlled release of cephalexin, Med. Chem. 9 (2013) 672–680.
[29] S.S. Román, G. Nuno Almeida, M. del Arco, C. Martín, Dexketoprofen and aceclofenac release from layered double hydroxide and SBA-15 ordered mesoporous material, Appl. Clay Sci. 121–122 (2016) 9–16.
[30] S. Jangra, S. Devi, V.K. Tomer, V. Chhokar, S. Duhan, Improved antimicrobial property and controlled drug release kinetics of silver sulfadiazine loaded ordered mesoporous silica, J. Asian Ceram. Soc. 4 (2016) 282–288.
[31] A. Salis, M.S. Bhattacharyya, M. Monduzzi, Specific ion effects on adsorption of lyso-zyme on functionalized SBA-15 mesoporous silica, J. Phys. Chem. B 114 (2010) 7996–8001.
[32] P. Schmidt-Winkel, W.W. Lukens, P. Yang, D.I. Margolese, J.S. Lettow, J.Y. Ying, G.D. Stucky, Microemulsion templating of siliceous mesostructured cellular foams with well-defined ultralarge mesopores, Chem. Mater. 12 (2000) 686–696.
[33] P. Schmidt-Winkel, W.W. Lukens, D. Zhao, P. Yang, B.F. Chmelka, G.D. Stucky, Mesocellular siliceous foams with uniformly sized cells and windows, J. Am. Chem. Soc. 121 (1999) 254–255.
[34] H. Gustafsson, E.M. Johansson, A. Barrabino, M. Odén, K. Holmberg, Immobilization of lipase from Mucor miehei and Rhizopus oryzae into mesoporous silica – the effect of varied size and morphology, Colloids Surf. B Biointerfaces 100 (2012) 22–30.
[35] L. Li, Y. Sun, B. Cao, H. Song, Q. Xiao, W. Yi, Preparation and performance of polyurethane/mesoporous silica composites for coated urea, Mater. Des. 99 (2016) 21–25.
[36] D. Zhao, Q. Huo, J. Feng, B.F. Chmelka, G.D. Stucky, Triblock Copolymer syntheses of mesoporous silica with periodic 50 to 300 angstrom pores, Science 279 (1998) 548–552.
[37] S. Brunauer, P.H. Emmet, E. Teller, Adsorption of gases in multimolecular layers, J. Am. Chem. Soc. 60 (1938) 309–319.
[38] J. Villarroel-Rocha, D. Barrera, K. Sapag, Introducing a self-consistent test and the corresponding modification in the Barrett, Joyner and Halenda method for pore-

size determination, Microporous Mesoporous Mater. 200 (2014) 68–78.
[39] S.K. Park, J.H. Kwon, The fate of two isothiazolinone biocides 5-chloro-2-methylisothiazol-3(2H)-one (CMI) and 2-methylisothiazol-3(2H)-one (MI), in liquid air fresheners and assessment of inhalation exposure, Chemosphere 144 (2016) 2270–2276.
[40] S. Lowell, J.E. Shields, M.A. Thomas, M. Thommes, Characterization of Porous Solids and Powders: Surface Area, Pore Size and Density, Kluwer Academic Publishers, 2003.
[41] M. Thommes, K. Kaneko, A.V. Neimark, J.P. Olivier, F. Rodriguez-Reinoso, J. Rouquerol, K.S.W. Sing, Physisorption of gases, with special reference to the evaluation of surface area and pore size distribution (IUPAC Technical Report), Pure Appl. Chem. 87 (2015) 1051–1069.
[42] M.S. Legnoverde, E.I. Basaldella, Influence of particle size on the adsorption and release of cephalexin encapsulated in mesoporous silica SBA-15. Equilibrium and kinetic studies, Mater. Lett. 181 (2016) 331–334.
[43] L.E. Mardones, M.S. Legnoverde, S. Simonetti, E.I. Basaldella, Theoretical and experimental study of isothiazolinone adsorption onto ordered mesoporous silica, Appl. Surf. Sci. 389 (2016) 790–796.
[44] M. Ghaedi, A. Ansari, R. Sahraei, ZnS:Cu nanoparticles loaded on activated carbon as novel adsorbent for kinetic, thermodynamic and isotherm studies of reactive orange 12 and direct yellow 12 adsorption, Spectrochim. Acta A 114 (2013) 687–694.
[45] D. Nityanandi, C.V. Subbhuraam, Kinetics and thermodynamics of adsorption of Cr (VI) from aqueous solution using puresorbe, J. Hazard. Mater. 170 (2009) 876–882.
[46] J. Febrianto, A.N. Kosasih, J. Sunarso, Y. Ju, N. Indraswati, S. Ismadji, Equilibrium and kinetic studies in adsorption of heavy metals using biosorbent: a summary of recent studie, J. Hazard Mater. 162 (2009) 616–645.
[47] S. Tunali, A.S. Ozcan, A. Ozcan, T. Gedikbey, Kinetics and equilibrium studies for the adsorption of Acid Red 57 from aqueous solutions onto calcined-alunite, J. Hazard. Mater. 35 (2006) 141–148.
[48] G. Bayramoglu, B. Altintas, M.Y. Arica, Adsorption kinetics and thermodynamic parameters of cationic dyes from aqueous solutions by using a new strong cation-exchange resin, Chem. Eng. J. 152 (2009) 339–346.
[49] S.M.L. Santos, J.A. Cecilia, E. Vilarrasa-García, I.J. Silva Junior, E. Rodríguez-Castellón, D.C.S. Azevedo, The effect of structure modifying agents in the SBA-15 for its application in the biomolecules adsorption, Microporous Mesoporous Mater. 232 (2016) 53–64.
[50] E.I. Basaldella, M.S. Legnoverde, Functionalized silica matrices for controlled delivery of cephalexin, J. Sol-Gel Sci. Technol. 56 (2010) 191–196.
[51] I. Izquierdo-Barba, M. Colilla, M. Manzano, M. Vallet-Regí, In vitro stability of SBA-15 under physiological conditions, Microporous Mesoporous Mater. 132 (2010) 442–452.
[52] G. Mille, J.L. Meyer, J. Chouteau, Δ-2 thiazoline et alkyl-2 Δ-2 thiazolines: étude vibrationnelle infrarouge et raman conformation, J. Mol. Struct. 50 (1978) 247–257.